

Document downloaded from:

<http://hdl.handle.net/10251/171224>

This paper must be cited as:

Silva Espinoza, MA.; Camacho Vidal, MM.; Martínez-Navarrete, N. (2020). Use of different biopolymers as carriers for purposes of obtaining a freeze-dried orange snack. *LWT - Food Science and Technology*. 127:1-7.
<https://doi.org/10.1016/j.lwt.2020.109415>



The final publication is available at

<https://doi.org/10.1016/j.lwt.2020.109415>

Copyright Elsevier

Additional Information

1 USE OF DIFFERENT BIOPOLYMERS AS CARRIERS FOR PURPOSES OF OBTAINING A
2 FREEZE-DRIED ORANGE SNACK

3

4 Marilu Andrea Silva-Espinoza, María del Mar Camacho, Nuria Martínez-Navarrete*

5 Food Technology Department, Food Investigation and Innovation Group, Universitat Politècnica de
6 València, Camino de Vera s/n, 46022, Valencia, Spain.

7 *Email: nmartin@tal.upv.es

8

9 Abstract

10 In addition to colour, one of the most important qualities of a snack-type product is its crunchy
11 texture. A freeze-dried fruit snack is characterised by its low water content, which creates the
12 problem of a loss of crunchiness related to its low glass transition temperature (Tg). In this sense, a
13 common technique with which to increase the Tg of these types of products is to add different
14 biopolymers. However, these compounds can, at the same time, affect the colour and texture of the
15 product. In this study, different biopolymers have been tested in order to discover their similarities or
16 differences in terms of hygroscopicity, antiplasticising character, colour and impact on the
17 mechanical properties of a freeze-dried orange snack formulated from their different mixtures. Gum
18 Arabic, maltodextrin, starch modified with octenylsuccinic anhydride, pea fibre, bamboo fibre and
19 native corn starch have been selected as biopolymers. The impact of any of them on the studied
20 properties can be confirmed, without any of them being more or less effective than the others.

21

22 Keywords: gum Arabic, maltodextrin, modified and native starch, pea and bamboo fibre,
23 crunchiness.

24

25 1. Introduction

26 The consumption of fruit is part of a healthy diet and it is recommended as a way of improving our
27 health and well-being (WHO, 2018). With the intention of promoting the consumption of fruit among
28 the population, there is continuous interest in offering consumers new products that stimulate this
29 consumption (Telis & Martínez-Navarrete, 2012). To this end, there exists the possibility of
30 obtaining a snack from freeze-dried orange puree.

31 The final water content of the freeze-dried fruit will condition its characteristics, especially its optical
32 and textural properties, and the expected shelf life under given conditions (Telis & Martínez-
33 Navarrete, 2012). During the processing of typical snacks, a low water content is determinant for
34 their characteristic brittleness, crispness or crunchiness. The plasticising effect of water on the
35 mechanical properties of the food systems is well known (Roos, 1995). The primary mechanical
36 effect of a plasticizer is that of weakening or breaking intermolecular bonds, thus decreasing its
37 mechanical resistance and increasing its deformability, gumminess or sogginess (Pittia & Sacchetti,
38 2008). The impact of water content change on the mechanical behaviour of a food has been related
39 to its physical state (Roos, 1995). Dehydrated fruits obtained by freeze-drying are normally in an
40 amorphous state. Above the glass transition temperature (T_g), the change from the glassy state,
41 more stable, to the rubbery occurs. The much lower viscosity of the rubbery state determines the
42 aforementioned product softening, so that the typical crunchiness is lost. For this reason, it is of
43 great importance to ensure the glassy state of a crispy product. To this end, it should be processed
44 and stored at temperatures below its T_g . Likewise, it is important to know, at a specified storage
45 temperature, the critical water content (CWC) and the critical water activity (CWA) of the product in
46 order to ensure the glassy state. As in the low water content range, a small increase in the food
47 water content leads to a significant decrease in the corresponding T_g , the storage relative humidity
48 (RH) has to be strictly controlled. The state diagram of a food is one tool with which to predict and
49 control the phase transitions. According to different authors, it is the right tool for the purposes of
50 finding out the relationships between T_g and the water content in order to design efficient processes
51 to obtain high-quality products and also to optimize storage conditions (Fabra, Talens, Moraga, &
52 Martínez-Navarrete, 2009; Rahman, 2006; Roos & Karel, 1991; Roos, 1995).

53 Freeze-dried fruit pulps, such as sugar-rich foods, present structural problems of stickiness, caking
54 and collapse. The T_g of freeze-dried fruit products present very low values, between 25 °C and -38
55 °C for a water content of between 3.3 and 25% (Telis & Martínez-Navarrete, 2010). Therefore, it is
56 fairly easy to find these products in a rubbery state under the usual storage conditions. One way to
57 prevent this, is, for example, the addition of biopolymers of high molecular weight that contribute to
58 increasing the value of T_g or that even play a steric role delaying the structural collapse.
59 Biopolymers, such as gums (gum Arabic, xanthan), maltodextrins, proteins (whey protein
60 concentrate), starches (octenyl succinic anhydride, waxy starch) and natural fibres (bamboo fibre),
61 have been used as drying carriers to obtain stable dehydrated products (Agudelo, Igual, Camacho,
62 & Martínez-Navarrete, 2017; Bhusari, Muzaffar, & Kumar, 2014; Cano-Chauca, Stringheta, Ramos,
63 & Cal-Vidal, 2005; Da Silva et al., 2013; Fongin, Kawai, Harnkarnsujarit, & Hagura, 2017; González,
64 García-Martínez, Camacho, & Martínez-Navarrete, 2019; Martínez-Navarrete, Salvador, Oliva, &
65 Camacho, 2019; Telis & Martínez-Navarrete, 2009). However, the addition of biopolymers may
66 cause unintended effects in other properties, such as changes in the colour or texture of the final
67 product. Non-enzymatic browning reactions, such as Maillard reactions and caramelization, may
68 stem from heating or occur during the long-term storage of foods containing carbohydrates,
69 especially reducing sugars (BeMiller & Whistler, 1996; Telis & Martínez-Navarrete, 2012). Since the
70 biopolymers differ as to their composition and nature, their interactions with the food matrix may
71 vary, causing different water-solid interactions. According to Acevedo, Schebor, & Buera (2008),
72 there is a correlation of the effects of water-solid interactions and water mobility on the non-
73 enzymatic browning rates in freeze-dried potato. Some authors have studied the effect of different
74 storage vapour pressure atmospheres on the stability of fruit powders containing biopolymers. They
75 have found that the mechanical properties of the dried food are closely dependent on the a_w (Pérez-
76 Alonso, Beristain, Lobato-Calleros, Rodríguez-Huezo, & Vernon-Carter, 2006; Telis & Martínez-
77 Navarrete, 2009).

78 In this study, different biopolymers, gum Arabic, maltodextrin, starch modified with octenylsuccinic
79 anhydride, pea fibre, bamboo fibre and native corn starch, have been tested in order to evaluate the

80 possible advantages or disadvantages of each one of them when added to an orange puree for the
81 purposes of freeze-drying and obtaining a snack.

82 2. Materials and Methods

83 2.1. Raw materials

84 2.1.1. Fruit

85 The oranges (*Citrus x sinensis* var. Navel) used in this study were bought from a local supermarket
86 in the city of Valencia (Spain). The fruit pieces were chosen by visual inspection based on the size,
87 homogeneity, colour and good physical integrity.

88 2.1.2. Biopolymers

89 The carriers used to obtain the dehydrated orange samples were gum Arabic (GA, Scharlab,
90 Sentmenat, Spain), maltodextrin (MD, Roquette, France), starch modified with octenylsuccinic
91 anhydride (OSA, Roquette, France), pea fibre (PF, Roquette, France), native corn starch (NC,
92 Roquette, France) and bamboo fibre (BF, VITACEL®, Germany). These biopolymers were selected
93 to avoid structural collapse of the dehydrated product, GA, MD and OSA for its ability to increase T_g
94 and BF, NCS and PF because of its steric role avoiding the formation of interparticle bridges.

95 2.2. Samples preparation

96 In order to obtain the orange puree, the fruit was washed, peeled, cut and triturated in a bench top
97 electrical food processor for 40 s at speed 4 (2000 rpm) followed by 40 s at speed 9 (91000 rpm)
98 (Thermomix TM 21, Vorwerk, Spain). The orange puree was mixed (10 min at speed 3 (1000 rpm)
99 with the biopolymers (Table 1) to obtain five different formulated samples to be freeze-dried, in
100 addition to the orange puree with no biopolymers (O) that was also considered. The ratio orange
101 puree:biopolymers was selected to ensure the physical stability of the dried product (Agudelo, Igual,
102 Camacho, & Martínez-Navarrete, 2017).

103 For freeze-drying purposes, each of the samples was distributed on two aluminium plates, 10.5 x
104 7.8 cm, 0.5 cm thickness, and immediately frozen at -45 °C (Liebherr LGT 2325, Germany) and
105 then dried (Telstar Lioalfa-6, Spain), at 0.05 mbar, -45 °C on the condenser and 40 °C on the

106 shelves for 20 hours, to obtain two cakes from each of the six different freeze-dried cakes (O,
107 GA+BF, MD+PF, MD+NCS, OSA+PF, OSA+NCS). One cake from each sample was crushed
108 manually with a mortar to obtain the corresponding powder.

109 2.3. Sorption experiments

110 The freeze-dried cake and the powder from each of the six samples were placed at 20 °C in
111 hermetic chambers containing saturated salt solutions (BrLi, ClLi, CH₃COOK, MgCl₂, K₂CO₃,
112 Mg(NO₃)₂, the corresponding relative humidity (RH) ranging between 6% and 53% (Greenspan,
113 1977). The samples were weighed every week in order to determine the equilibrium condition with
114 the surroundings ($\Delta m < \pm 0.001$ g) (Kaymak-Ertekin & Gedik, 2004). In this moment, the water activity
115 of each sample was assumed to be equal to the corresponding RH/100. The time needed to reach
116 equilibrium was approximately two months.

117 2.4. Analytical determination

118 2.4.1. Water content (x_w)

119 The mass fraction of water (x_w) was obtained by drying the equilibrated powdered samples in a
120 vacuum oven (Selecta®, Vaciotem-T, J.P. Selecta S.A., Spain) at 60°C ± 1°C under $p < 100$ mm Hg
121 until constant weight (AOAC, 1990). Three replicates were carried out on each of the six
122 equilibrated freeze-dried samples and the mean value was considered as the corresponding x_w .

123 2.4.2. Glass transition temperature (T_g)

124 The T_g of the powdered samples conditioned at different water contents was determined by
125 differential scanning calorimetry (DSC 220CU-SSC5200, Seiko instruments Inc., Japan).
126 Approximately 15 mg of each sample were placed into DSC pans (P/N SSC000C008, Seiko
127 Instruments Inc., Japan). The heating rate was 5 °C/min and the temperature range varied between
128 -80 °C and 80 °C, depending on the water activity of each sample. The onset, midpoint and
129 endpoint of the glass transition were obtained from each thermogram.

130 2.4.3. Fitted models

131 In order to predict the water sorption behaviour of the samples, the linearized BET model (Eq. 1)
132 was used to predict water sorption up to $a_w \approx 0.5$ (Brunauer, Emmett & Teller, 1938).

133

$$134 \quad \frac{a_w}{(1-a_w) W_e} = \frac{1}{W_0 C} + \frac{C-1}{W_0 C} \cdot a_w \quad (1)$$

135

136 Where W_e is the equilibrium water content (g water/g dry solute), W_0 is the monolayer water content
137 value (g water/g dry solute), C is the energy constant related to the sorption heat and a_w is the water
138 activity.

139

140 In order to predict glass transition temperatures, experimental $T_g - x_w$ data were fitted to the
141 linearized Gordon & Taylor (1952) equation (Eq. 2) considering the onset, midpoint and end of the
142 transition.

143

$$144 \quad T_g = T_{g(s)} + k \frac{x_w \cdot (T_{g(w)} - T_g)}{(1-x_w)} \quad (2)$$

145

146 Where T_g is the glass transition temperature ($^{\circ}\text{C}$), $T_{g(s)}$ is the glass transition temperature of the
147 anhydrous solids ($^{\circ}\text{C}$), k is the Gordon y Taylor constant model, x_w is the mass fraction of water (g
148 water/g product) and $T_{g(w)}$ is the glass transition temperature of amorphous water: -135°C (Roos,
149 1995).

150

151 The relationship between $T_g - a_w$ is given by the linear regression proposed by Roos (1995) (Eq. 3),
152 where Y and Z are the constants of the model.

153

$$154 \quad T_g = Y a_w + Z \quad (3)$$

155 2.4.4. Mechanical properties

156 The mechanical behaviour of the equilibrated samples was registered using a texture analyser TA-
157 XT2i (Stable Micro Systems, UK). Portions of 20 x 20 mm of the freeze-dried cakes were

158 compressed using a cylindrical probe of 10 mm diameter applying a strain of 80% with a test speed
159 of 1 mms⁻¹. Five replicates were performed per sample. The parameters analysed in the test were
160 the maximum force (F), expressed in Newtons.

161 2.4.5. Colour measurements

162 CIE L*a*b* colour space was selected as a uniform and objective method with which to specify the
163 colour of equilibrated freeze-dried cake samples. The L* coordinate denotes lightness on a 0–100
164 scale from black to white; a*, (+) red or (-) green; b*, (+) yellow or (-) blue. Colour coordinates (10°
165 observer and D65 illuminant) were obtained from the reflectance spectrum using a
166 spectrophotometer (Minolta, CM 3600D, Japan). The colour was measured at four different points
167 of the whole cake and the mean value was considered. From the colour coordinates, the hue angle
168 (h*, Eq. 4), and chroma or saturation (C*, Eq. 5) were obtained. Measurements were taken with the
169 specular component excluded.

170

$$171 \quad h^* = \arctg(b^*/a^*) \quad (4)$$

172

$$173 \quad C^* = (a^{*2} + b^{*2})^{0.5} \quad (5)$$

174

175 3. Results and Discussion

176 3.1. Sorption behaviour

177 The obtained sorption isotherms predict the relationship between w_e and a_w of the different freeze-
178 dried orange purees at 20 °C (Fig. 1). As can be observed, all the added biopolymers reduced the
179 hygroscopicity of the orange cake over the whole a_w range of, OSA seeming to be the most
180 effective for this purpose.

181 The experimental data of each sample were fitted to the BET model (Table 2). The BET monolayer
182 water content (W_o) was in the range of 0.0619 – 0.0742 g water/g dry solid, the highest value being
183 that of the orange sample without biopolymers and the lowest that of the orange with OSA ones.
184 The W_o indicates the amount of water that is tightly adsorbed in specific sites on food surfaces,

185 which has been related with a security water content below which the product stability is guaranteed
186 (Choudhury, Sahu, & Sharma, 2011; Telis & Martínez-Navarrete, 2010; Wan et al., 2018). The
187 values of constant C, the other BET parameter, varied between 2.25 – 2.96, which allows these
188 sorption isotherms to be classified as type II (Brunauer, Deming, Deming & Teller, 1940). In order to
189 evaluate the significant differences in the sample's sorption behaviour, the BET equation fitted to
190 each sample and that fitted to different groups of samples were statistically compared through the
191 values of the statistic E, which was compared with tabulated F – Snedecor (Moraga et al., 2004).
192 The obtained results permitted a twofold confirmation: that there were no differences between the
193 formulated samples ($P>0.05$) and that all of them were different to the O sample ($P<0.05$). In this
194 way, the capacity of any of the biopolymers used to reduce the hygroscopicity of the freeze-dried
195 orange snack can be confirmed, without any of them being more or less effective than the others.

196

197 3.2. Glass transition temperature- water content-water activity relationships

198 The glass transition temperature of dried foods is extremely important as a means of predicting the
199 conditions of a proper drying process and product storage (Roos & Karel, 1991). Nevertheless,
200 glass transition is a state transition that is developed over a temperature range. That is why the
201 onset (Tg^o), mid-point (Tg^m) and end-point (Tg^e) of glass transition can be characterized (Fig. 2).
202 The majority of studies published take Tg^m as the characteristic Tg value (Goula, Karapantsios,
203 Achilias, & Adamopoulos, 2008; Khallooufi & Ratti, 2003; Roos, 1995; Wu, Sun, & Liu, 2019).
204 However, the change in the food properties associated with glass transition, could start from the
205 moment in which the transition begins or might not become patent until the entire amorphous matrix
206 has changed to the rubbery state, at the end of the Tg. For this reason, it may be interesting to
207 consider Tg^o and Tg^e as being related to the physical properties (Rahman, 2006; Wan et al., 2018).
208 The samples considered in this study showed a Tg amplitude of about 5-15 °C and, as expected,
209 the Tg fell as the water content increased (Fig. 2). The orange sample without biopolymers
210 presented lower Tg values than the samples with added biopolymers, especially in the lower water
211 content range (approximately up to 0.07g water/g product). From this value, the added biopolymers
212 do not seem to have so much influence on the Tg. The GA+BF sample seems to be the one that

213 most increases the T_g over the entire water content range. Each one of the 3 characteristic values
214 of the T_g of each sample was related to the corresponding water content by fitting the Gordon and
215 Taylor model (Eq. 2). Table 3 shows the corresponding k and $T_{g(s)}$ parameters. The value of these
216 parameters confirms the above comments. In this sense, the lowest $T_{g(s)}$ was that of the O sample
217 and the highest that of the GA+BF sample, the amplitude of the corresponding T_g ranging between
218 7.6 and 14.7 °C, respectively. Again, the statistical comparison among the different Gordon and
219 Taylor fittings, performed through comparing the values of statistic E with the tabulated F-Snedecor,
220 showed that only the O sample was different as regards the water plasticization behaviour. No
221 significant differences ($P>0.05$) were detected among the formulated samples.

222 As shown in Fig. 1, T_g - a_w - w_e relationships may be plotted together to construct the stability map,
223 which is a tool that permits an easy identification of the critical processing or storage conditions
224 (temperature and relative humidity) for glass transition (Fabra et al., 2009). Table 4 shows the
225 critical water content (CWC) and critical water activity (CWA) values that have to be exceeded for
226 the glass transition to take place, both at 20 and 4 °C, common room and refrigeration
227 temperatures. The freeze-dried orange cake with added biopolymers showed higher values of CWC
228 and CWA than the O sample, related to the greater capacity of these samples to maintain the more
229 stable glassy state. It is remarkable that, despite the great microbiological and chemical stability of
230 the dehydrated products, decreasing the storage temperature appreciably increases the CWC and
231 CWA of all the samples. In this regard, at 20 °C for instance, the glass transition of the GA+BF
232 sample will take place, at a surrounding RH in the range of 19.0-30.2%, this increasing to 31.1-
233 42.5% at 4 °C. This increase in the critical values may be related to the physical stability of the
234 products in terms of aspects such as the texture or colour of the snack.

235 On the other hand, in order to obtain a tool that makes it easy to relate both temperature and RH
236 storage conditions for glass transition, T_g and a_w were related using the linear relationship (Eq. 3)
237 proposed by Roos (1995). Table 2 shows the results of this fit, where a very good and useful linear
238 relationship can be observed.

239

240 3.3. Colour and mechanical properties

241 The addition of biopolymers led to an increase in L^* and a decrease in a^* and b^* , so that the
242 chroma of the samples decreased and the hue angle increased (Fig. 3). This colour change is
243 related to the colour of the biopolymers themselves and to the dilution of the orange pigments in the
244 formulated samples (Telis & Martínez-Navarrete, 2009). The whitish colour of the biopolymers
245 contributes to the increase in lightness, the colour becoming yellower and less pure. The most
246 significant colour change in every sample was observed at water activities between 0.328 and
247 0.432. At this a_w , the amorphous matrices of all the samples are already in a totally rubbery state
248 (Table 4), and the water content is enough for enzymatic and non-enzymatic oxidation and
249 browning reactions to occur. From this water activity, the greater amount of water present in the
250 samples exerts a dilution effect of the components responsible for the colour, which means that the
251 change in colour is no longer so marked.

252 The variation in the mechanical properties of the studied snacks was evaluated from the force–
253 deformation curves. Fig. 4 shows the typical shape of the force–distance curves obtained from the
254 different studied samples with several a_w . For the purposes of clarity, only one of the replicates at
255 each a_w was selected for the Figure. In every case, the increase in the water content dramatically
256 affected the shape of the curve, so that a change from a jagged to a smooth and regular trend of
257 the force–deformation relationship was observed. This change is related to the material
258 transformation from hard and brittle (or crunchy and crispy) when dried to soft and ductile at a
259 higher water content (Martínez-Navarrete et al., 2019). The loss of crispness in the orange sample
260 without added biopolymers was evident at water activities between 0.113 and 0.225, while in the
261 samples with added biopolymers it was in the range of 0.225–0.328. In every case, the number of
262 fracture peaks observed at the lower a_w decreased when the water content rose. These results
263 point to the fact that any of the studied biopolymers may be used to protect the mechanical
264 properties of the snack over a wider water content range, although there is still a limit to the gain of
265 water if the quality of the product is to be ensured.

266 As a measurement of the strength of the samples with different a_w and so different water contents,
267 the maximum force achieved in the mechanical test (F_{max}) was characterized from the force–
268 distance curves (Fig. 5). Significant differences ($p < 0.05$) were observed between samples and a_w .

269 In order to confirm the impact of the physical state of the snack matrix on the measured mechanical
270 response, the CWA for the glass transition of every sample (Table 4) was related with Fmax. Fig. 5
271 shows CWA for the onset and end point of the Tg (CWA^o and CWA^e , respectively) of the O and
272 GA+BF samples, and also those of the OSA+PF sample, whose values were genuinely close to the
273 rest of the samples. As may be observed, the values of Fmax remain low below CWA^o , while all the
274 product matrix is in the glassy state. Fmax sharply increases while the transition from the glassy to
275 the rubbery state occurs (between CWA^o and CWA^e) and sharply decreases again when the
276 rubbery state is fully achieved, above CWA^e . The small differences observed in the Tg- x_w - a_w
277 relationships of the different samples containing biopolymers, despite not being significant ($P>0.05$),
278 were enough to ensure a significantly ($P<0.05$) higher Fmax value of the GA+BF sample at $a_w =$
279 0.328 compared to the other samples, MD+PF having intermediate values.

280 The decrease in Fmax is related with the plasticizing effect of water in the fully rubbery state. In this
281 state, the amount of water in the sample is enough to ensure all the primary interactions with the
282 matrix and there is still water available to contribute to the softening of the sample by weakening
283 intermolecular bonds. The increase in Fmax at the lowest a_w , also observed in other studies
284 (Chang, Cheah, & Seow, 2000; Moraga, Talens, Moraga, & Martínez-Navarrete, 2011; Sogabe,
285 Kawai, Kobayashi, Jothi, & Hagura, 2018), has been called the anti-plasticization effect of water
286 and it has been related with an increase in the cohesiveness of the glassy food matrix that
287 increases its rigidity and firmness (Pittia & Sacchetti, 2008). This offers a greater resistance upon
288 force application and more energy is needed to compress the sample. For these authors, the anti-
289 plasticization effect could be considered as a mere hardening or 'toughening' effect. This hardening
290 limit the number of fractures when a_w increases over this low a_w range. In fact, it seems that the loss
291 in the number of observed multiple fracture peaks occurs at the same a_w from which Fmax starts to
292 decrease (Figs 4-c and 5), when the whole matrix is in the rubbery state.

293 The above results indicate the need to keep the orange snack in a completely glassy state to
294 ensure a crispy texture and adequate colour. Despite the fact that the W_o value has frequently been
295 considered as a secure water content below which product stability is guaranteed (Choudhury et al.,
296 2011; Telis & Martínez-Navarrete, 2010; Wan et al., 2018), in this study, the CWC that ensured the

297 glassy state of the studied snack was lower than W_o (Tables 2 and 4). In this sense, regardless of
298 whether W_o may be considered an optimum value for the purposes of preventing processes such as
299 oxidative deterioration (Goula et al., 2008), it is not only a_w but also T_g data that may be considered
300 as complementary tools with which to ensure the stability of some products.

301 4. Conclusions

302 Any of the biopolymers studied permit a reduction in hygroscopicity and an increase in the glass
303 transition temperature of the freeze-dried orange snack, without any of them being more or less
304 effective than the others. The typical crunchy characteristics of the snack are lost at the onset of
305 glass transition, while the colour changes are evident at its end. This indicates the need to keep the
306 snack at temperatures below its T_g , depending on its water content. In this sense, it is
307 recommended that the orange puree be formulated with any of the biopolymers studied and,
308 although unnecessary from the perspective of chemical and microbiological stability, stored in
309 refrigeration.

310 5. Acknowledgments

311 The authors thank the Ministerio de Economía y Competitividad for the financial support given
312 through the Project AGL 2017-89251 and the Ministerio de Educación for the FPU grant (FPU14 /
313 02633) awarded to Ms. Andrea Silva.

314 6. References

- 315 Acevedo, N. C., Schebor, C., & Buera, P. (2008). Non-enzymatic browning kinetics analysed
316 through water-solids interactions and water mobility in dehydrated potato. *Food Chemistry*, *108*,
317 900–906. <https://doi.org/10.1016/j.foodchem.2007.11.057>
- 318 Agudelo, C., Igual, M. M., Camacho, M. M., & Martínez-Navarrete, N. (2017). Effect of process
319 technology on the nutritional, functional, and physical quality of grapefruit powder. *Food Science
320 and Technology International*, *23*, 61–74. <https://doi.org/10.1177/1082013216658368>
- 321 AOAC (1990). *Official methods of analysis of AOAC International* (15th ed.). Arlington: Association
322 of Official Analytical Chemists

- 323 BeMiller, J. N. & Whistler, R. L. (1996). Carbohydrates. In O. R. Fenemma (Eds.), *Food Chemistry*,
324 3rd edition (pp. 157–224). New York: Marcel Dekker.
- 325 Bhusari, S. N., Muzaffar, K., & Kumar, P. (2014). Effect of carrier agents on physical and
326 microstructural properties of spray dried tamarind pulp powder. *Powder Technology*, 266, 354–
327 364. <https://doi.org/10.1016/j.powtec.2014.06.038>
- 328 Brunauer, S., Emmett, P.H., Teller, E. (1938). Adsorption of gases in multimolecular layers. *Journal*
329 *of American Chemistry Society*, 60 , 309–320. <https://doi.org/10.1021/ja01269a023>
- 330 Brunauer, S., Deming, L.S., Deming, W.E., Teller, E. (1940). On a theory of the van de Waals
331 adsorption of gases. *Journal of American Chemistry Society*, 62, 1723–1732.
332 <https://doi.org/10.1021/ja01864a025>
- 333 Cano-Chauca, M., Stringheta, P. C., Ramos, A. M., & Cal-Vidal, J. (2005). Effect of the carriers on
334 the microstructure of mango powder obtained by spray drying and its functional characterization.
335 *Innovative Food Science and Emerging Technologies*, 6, 420–428.
336 <https://doi.org/10.1016/j.ifset.2005.05.003>
- 337 Chang, Y. P., Cheah, P. B., & Seow, C. C. (2000). Plasticizing – Antiplasticizing Effects of Water on
338 Physical Properties of Tapioca. *Journal of Food Science*, 65, 445–451.
339 <https://doi.org/10.1111/j.1365-2621.2000.tb16025.x>
- 340 Choudhury, D., Sahu, J. K., & Sharma, G. D. (2011). Moisture sorption isotherms, heat of sorption
341 and properties of sorbed water of raw bamboo (*Dendrocalamus longispathus*) shoots. *Industrial*
342 *Crops and Products*, 33, 211–216. <https://doi.org/10.1016/j.indcrop.2010.10.014>
- 343 Da Silva, F. C., Da Fonseca, C. R., De Alencar, S. M., Thomazini, M., Balieiro, J. C. D. C., Pittia, P.,
344 & Favaro-Trindade, C. S. (2013). Assessment of production efficiency, physicochemical
345 properties and storage stability of spray-dried propolis, a natural food additive, using gum Arabic
346 and OSA starch-based carrier systems. *Food and Bioproducts Processing*, 91, 28–36.
347 <https://doi.org/10.1016/j.fbp.2012.08.006>

348 Fabra, M. J., Talens, P., Moraga, G., & Martínez-Navarrete, N. (2009). Sorption isotherm and state
349 diagram of grapefruit as a tool to improve product processing and stability. *Journal of Food*
350 *Engineering*, 93, 52–58. <https://doi.org/10.1016/j.jfoodeng.2008.12.029>

351 Fongin, S., Kawai, K., Harnkarnsujarit, N., & Hagura, Y. (2017). Effects of water and maltodextrin on
352 the glass transition temperature of freeze-dried mango pulp and an empirical model to predict
353 plasticizing effect of water on dried fruits. *Journal of Food Engineering*, 210, 91–97.
354 <https://doi.org/10.1016/j.jfoodeng.2017.04.025>

355 González, F., García-Martínez, E., Camacho, M. del M., & Martínez-Navarrete, N. (2019). Stability
356 of the physical properties, bioactive compounds and antioxidant capacity of spray-dried
357 grapefruit powder. *Food Bioscience*, 28, 74–82. <https://doi.org/10.1016/j.fbio.2019.01.009>

358 Gordon, M., Taylor, J.S., (1952). Ideal copolymers and second-order transitions of synthetic
359 rubbers. I. Non-crystalline copolymers. *Journal of Applied Chemistry*, 2, 493–500.

360 Goula, A. M., Karapantsios, T. D., Achilias, D. S., & Adamopoulos, K. G. (2008). Water sorption
361 isotherms and glass transition temperature of spray dried tomato pulp. *Journal of Food*
362 *Engineering*, 85, 73–83. <https://doi.org/10.1016/j.jfoodeng.2007.07.015>

363 Greenspan, L. (1977). Humidity fixed point of binary saturated aqueous solutions. *Journal of*
364 *Research of the National Bureau of Standards-a Physics and Chemistry*, 81a, 89–96.

365 Kaymak-Ertekin, F., & Gedik, A. (2004). Sorption isotherms and isosteric heat of sorption for
366 grapes, apricots, apples and potatoes. *LWT - Food Science and Technology*, 37, 429–438.
367 <https://doi.org/10.1016/j.lwt.2003.10.012>

368 Khallooufi, S., & Ratti, C. (2003). Quality Deterioration of Freeze-dried Foods as Explained by their
369 Glass Transition. *Food Engineering and Physical Properties*, 68, 892-903.
370 <https://doi.org/10.1111/j.1365-2621.2003.tb08262.x>

371 Martínez-Navarrete, N., Salvador, A., Oliva, C., & Camacho, M. M. (2019). Influence of
372 biopolymers and freeze-drying shelf temperature on the quality of a mandarin snack. *LWT*, 99,

373 57–61. <https://doi.org/10.1016/j.lwt.2018.09.040>

374 Moraga, G., Martínez-Navarrete, N., & Chiralt, A. (2004). Water sorption isotherms and glass
375 transition in strawberries: Influence of pretreatment. *Journal of Food Engineering*, *62*, 315–321.
376 [https://doi.org/10.1016/S0260-8774\(03\)00245-0](https://doi.org/10.1016/S0260-8774(03)00245-0)

377 Moraga, G., Talens, P., Moraga, M. J., & Martínez-Navarrete, N. (2011). Implication of water activity
378 and glass transition on the mechanical and optical properties of freeze-dried apple and banana
379 slices. *Journal of Food Engineering*, *106*, 212–219.
380 <https://doi.org/10.1016/j.jfoodeng.2011.05.009>

381 Pérez-Alonso, C., Beristain, C. I., Lobato-Calleros, C., Rodríguez-Huezo, M. E., & Vernon-Carter, E.
382 J. (2006). Thermodynamic analysis of the sorption isotherms of pure and blended carbohydrate
383 polymers. *Journal of Food Engineering*, *77*, 753–760.
384 <https://doi.org/10.1016/j.jfoodeng.2005.08.002>

385 Pittia, P., & Sacchetti, G. (2008). Antiplasticization effect of water in amorphous foods. A review.
386 *Food Chemistry*, *106*, 1417–1427. <https://doi.org/10.1016/j.foodchem.2007.03.077>

387 Rahman, M. S. (2006). State diagram of foods: Its potential use in food processing and product
388 stability. *Trends in Food Science and Technology*, *17*, 129–141.
389 <https://doi.org/10.1016/j.tifs.2005.09.009>

390 Roos, Y.H. (1995). *Phase Transitions in Food*. San Diego: Academic Press.

391 Roos, Y., & Karel, M. (1991). Plasticizing effect of water on thermal behavior and crystallization of
392 amorphous food models. *Journal of Food Science*, *56*, 38–43. [https://doi.org/10.1111/j.1365-](https://doi.org/10.1111/j.1365-2621.1991.tb07970.x)
393 [2621.1991.tb07970.x](https://doi.org/10.1111/j.1365-2621.1991.tb07970.x)

394 Sogabe, T., Kawai, K., Kobayashi, R., Jothi, J. S., & Hagura, Y. (2018). Effects of porous structure
395 and water plasticization on the mechanical glass transition temperature and textural properties of
396 freeze-dried trehalose solid and cookie. *Journal of Food Engineering*, *217*, 101–107.
397 <https://doi.org/10.1016/j.jfoodeng.2017.08.027>

- 398 Telis, V. R.N., & Martínez-Navarrete, N. (2009). Collapse and color changes in grapefruit juice
399 powder as affected by water activity, glass transition, and addition of carbohydrate polymers.
400 *Food Biophysics*, 4, 83–93. <https://doi.org/10.1007/s11483-009-9104-0>
- 401 Telis, V. R.N., & Martínez-Navarrete, N. (2010). Application of compression test in analysis of
402 mechanical and color changes in grapefruit juice powder as related to glass transition and water
403 activity. *LWT*, 43, 744–751. <https://doi.org/10.1016/j.lwt.2009.12.007>
- 404 Telis, Vânia Regina Nicoletti, & Martínez-Navarrete, N. (2012). *Biopolymer Engineering in Food*
405 *Processing* (1st ed.). Florida: CRC Press, (Chapter 8).
- 406 Wan, J., Ding, Y., Zhou, G., Luo, S., Liu, C., & Liu, F. (2018). Sorption isotherm and state diagram
407 for indica rice starch with and without soluble dietary fiber. *Journal of Cereal Science*, 80, 44–49.
408 <https://doi.org/10.1016/j.jcs.2018.01.003>
- 409 WHO. Healthy Diet (2019). <https://www.who.int/news-room/fact-sheets/detail/healthy-diet> Accessed
410 15 July 2019.
- 411 Wu, H. Y., Sun, C. B., & Liu, N. (2019). Effects of different cryoprotectants on microemulsion freeze-
412 drying. *Innovative Food Science and Emerging Technologies*, 54, 28–33.
413 <https://doi.org/10.1016/j.ifset.2018.12.007>

414

415 **Figure captions**

416 Figure 1. Water content (w_e) - water activity (a_w) – onset glass transition temperature (T_g^0)
417 relationships of freeze-dried orange puree (O) and that formulated with: starch modified with
418 octenylsuccinic anhydride and native corn starch (OSA+NCS) or pea fibre (OSA+PF); maltodextrin
419 with native corn starch (MD+NCS) or pea fibre (MD+PF); gum Arabic with bamboo fibre (GA+BF).
420 The continuous lines represent the T_g - a_w fitted model, the discontinuous lines predict x_w - a_w data
421 obtained from the BET fitted model and the points correspond to experimental data. The black
422 dashed lines show, for the O sample, how to obtain the critical water activity and water content
423 (CWA and CWC, respectively) for glass transition at 20°C.

424 Figure 2. Mid-point glass transition temperature (Tg^m)-water content (x_w) relationship of freeze-dried
425 orange puree (O) and that formulated with: starch modified with octenylsuccinic anhydride and
426 native corn starch (OSA+NCS) or pea fibre (OSA+PF); maltodextrin with native corn starch
427 (MD+NCS) or pea fibre (MD+PF); gum Arabic with bamboo fibre (GA+BF). The lines represent the
428 Gordon and Taylor fitted model and the points correspond to experimental data. The inner graph
429 shows an example of one of the DSC thermograms obtained with GA+BF sample with $a_w = 0.06$.
430 The dashed lines and arrows indicate the way to obtain the temperature at the onset (Tg^0), mid-
431 point (Tg^m) and end-point (Tg^e) of glass transition.

432 Figure 3. Values of a) luminosity (L^*), b) chroma (C^*) and c) hue angle (h^*) of freeze-dried **snack**
433 **obtained from** orange puree (O) and that formulated with: starch modified with octenylsuccinic
434 anhydride and native corn starch (OSA+NCS) or pea fibre (OSA+PF); maltodextrin with native corn
435 starch (MD+NCS) or pea fibre (MD+PF); gum Arabic with bamboo fibre (GA+BF), conditioned at
436 different water activity (a_w).

437 Figure 4. Force (F) – distance (d) curves obtained with freeze-dried **snack obtained from** orange
438 puree (O) and that formulated with: starch modified with octenylsuccinic anhydride and native corn
439 starch (OSA+NCS) or pea fibre (OSA+PF); maltodextrin with native corn starch (MD+NCS) or pea
440 fibre (MD+PF); gum Arabic with bamboo fibre (GA+BF), conditioned at different water activity (a_w).

441 Figure 5. Values of maximum force (F_{max}) obtained in the mechanical test carried out with the
442 freeze-dried **snack obtained from** orange puree (O) and that formulated with: starch modified with
443 octenylsuccinic anhydride and native corn starch (OSA+NCS) or pea fibre (OSA+PF); maltodextrin
444 with native corn starch (MD+NCS) or pea fibre (MD+PF); gum Arabic with bamboo fibre (GA+BF),
445 conditioned at different water activity (a_w).

446

Table 1. Sample code as a function of the corresponding formulation.

Sample	Biopolymers added and concentration	
	5g/100 g orange puree	1g/100 g orange puree
GA+BF	gum Arabic	bamboo fibre
MD+PF	maltodextrin	pea fibre
MD+NC	maltodextrin	native corn starch
OSA+PF	starch modified with octenylsuccinic anhydride	pea fibre
OSA+NC	starch modified with octenylsuccinic anhydride	native corn starch

Table 2. Parameters of the BET (W_0 , C) and linear (Y, Z) models fitted to experimental water content-water activity (Eq. 1) and mid-point glass transition temperature-water activity (Eq. 3) data, respectively. The sample codes can be identified in Table 1.

Sample	C	W_0 (g water/g dry solids)	R^2	Y	Z	R^2
O	3,0	0,074	0,911	-124,4	36,8	0,981
OSA+PF	2,7	0,062	0,708	-137,8	51,9	0,969
OSA+NCS	2,8	0,062	0,837	-140,5	52,7	0,981
MD+PF	2,6	0,066	0,901	-130,4	49,3	0,982
MD+NCS	2,3	0,071	0,580	-136,2	50,9	0,985
GA+BF	2,8	0,066	0,827	-140,2	55,6	0,987

R^2 : adjusted determination coefficient

Table 3

Table 3. Gordon and Taylor parameters (K and Tgs) obtained when fitting the experimental onset, midpoint and end point of the glass transition temperature (Tg^0 , Tg^m and Tg^e , respectively) - water content relationship (Eq. 2). The sample codes can be identified in Table 1.

		O	OSA+PF	OSA+NCS	MD+PF	MD+NCS	GA+BF
Tg^0	K	5,69	6,93	7,24	6,16	6,52	6,62
	Tgs	37,2	48,6	50,6	45,1	47,7	52,6
	R^2	0,985	0,972	0,981	0,970	0,984	0,985
Tg^m	K	5,19	6,56	6,81	5,74	6,02	6,28
	Tgs	40,0	55,4	57,5	51,4	53,4	60,0
	R^2	0,958	0,963	0,982	0,964	0,989	0,988
Tg^e	K	4,86	6,22	6,44	5,36	5,56	5,97
	Tgs	44,8	62,3	64,4	57,8	59,2	67,3
	R^2	0,953	0,951	0,981	0,957	0,985	0,991

R^2 : adjusted determination coefficient

Table 4

Table 4. Values of the critical water content (CWC) and critical water activity (CWA) for the onset (^o) and end (^e) point of the glass transition at 20 and 4°C. The sample codes can be identified in Table 1.

		O	OSA+PF	MD+PF	OSA+NCS	MD+NCS	GA+BF
20 °C	CWA ^o	0,095	0,170	0,160	0,165	0,169	0,190
	CWA ^e	0,165	0,279	0,275	0,275	0,275	0,302
	CWC ^o	0,019	0,026	0,026	0,026	0,026	0,031
	CWC ^e	0,032	0,042	0,044	0,042	0,043	0,049
4 °C	CWA ^o	0,213	0,293	0,289	0,285	0,295	0,311
	CWA ^e	0,305	0,404	0,409	0,400	0,405	0,425
	CWC ^o	0,040	0,044	0,046	0,044	0,046	0,050
	CWC ^e	0,057	0,063	0,067	0,063	0,067	0,071

Figure 1

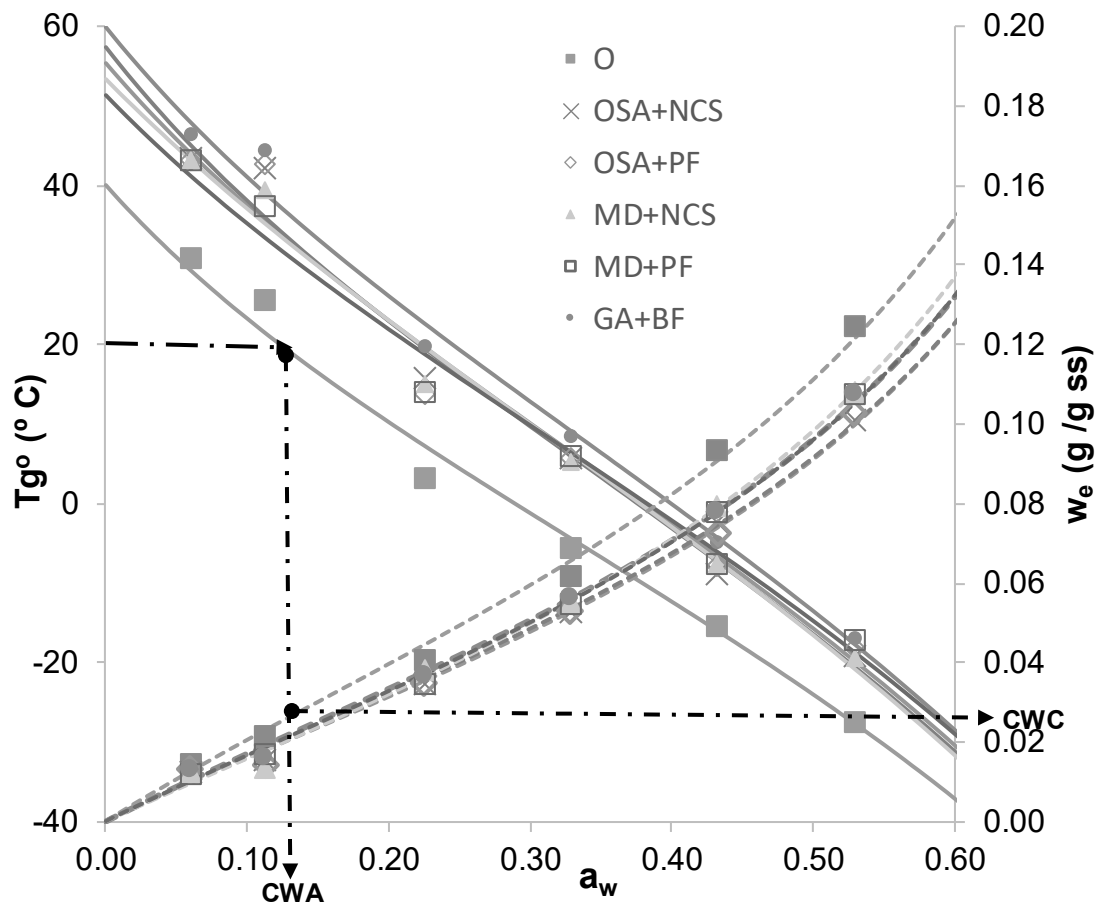


Figure 1

Figure 2

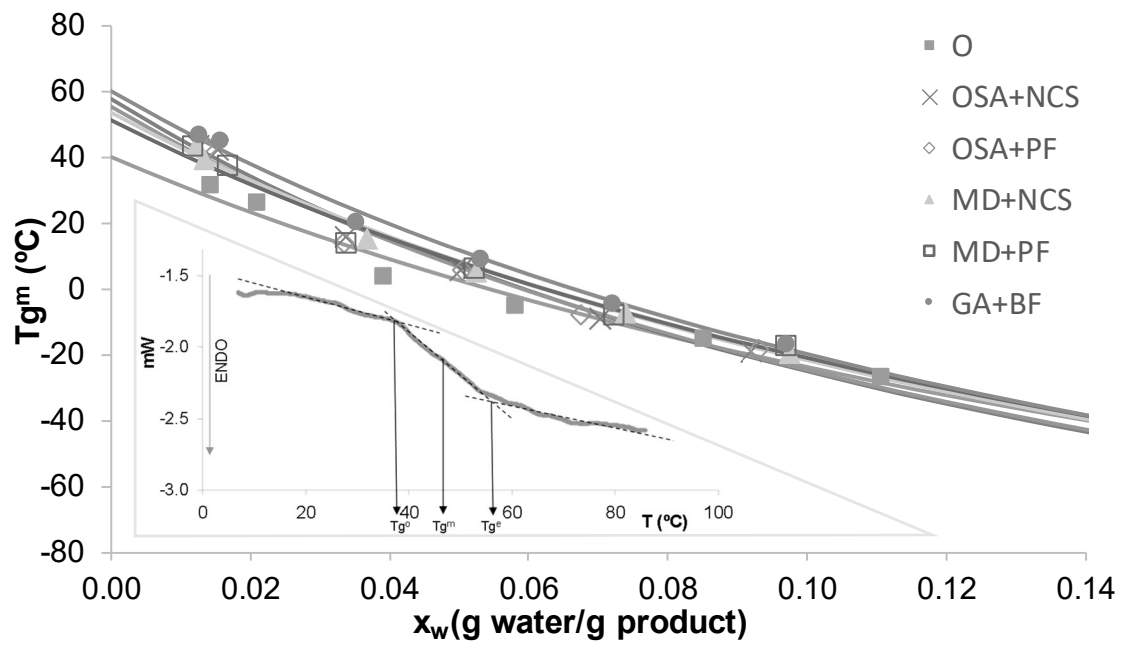


Figure 2

Figure 3

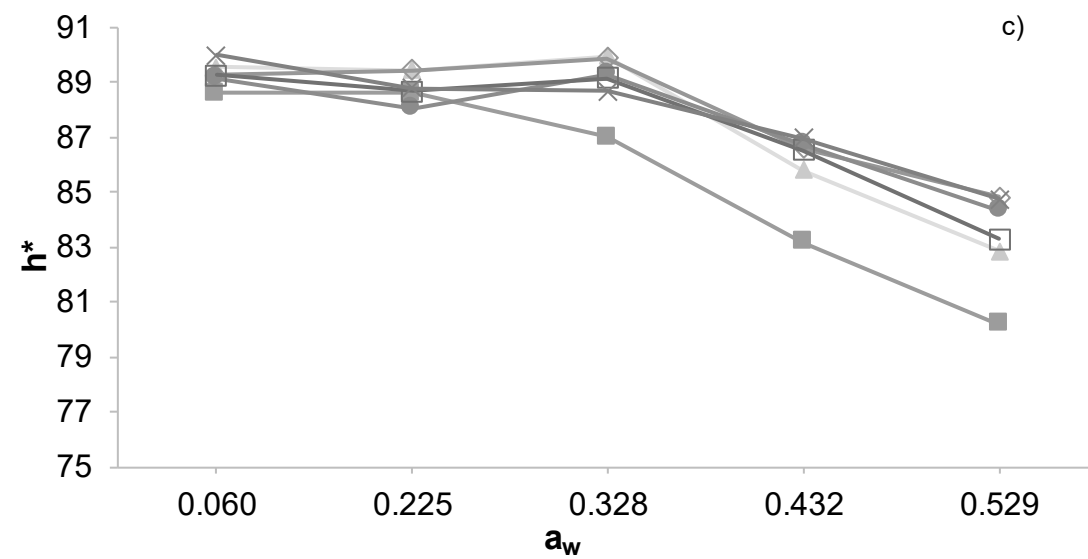
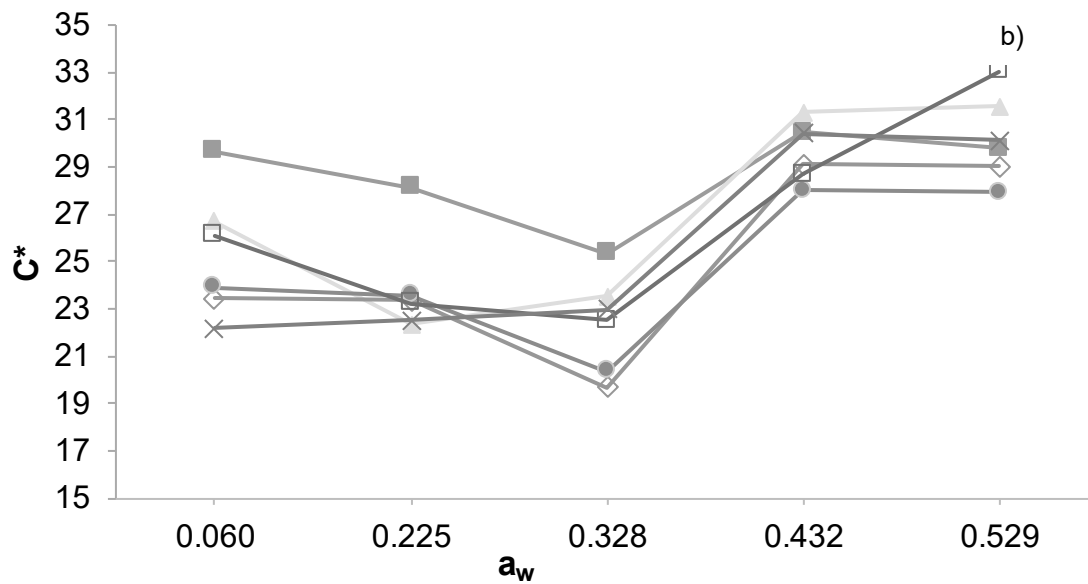
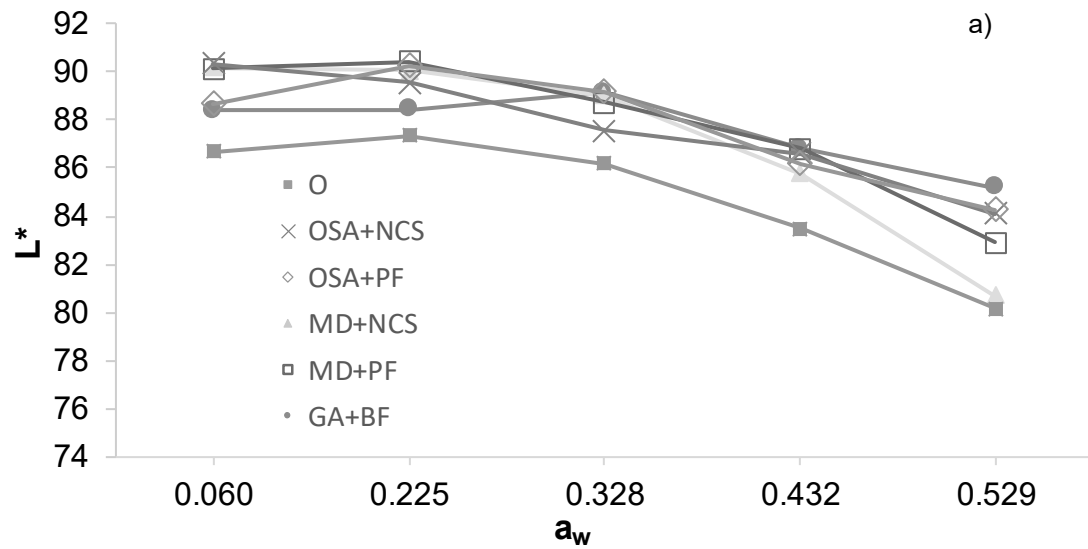


Figure 3

Figure 4

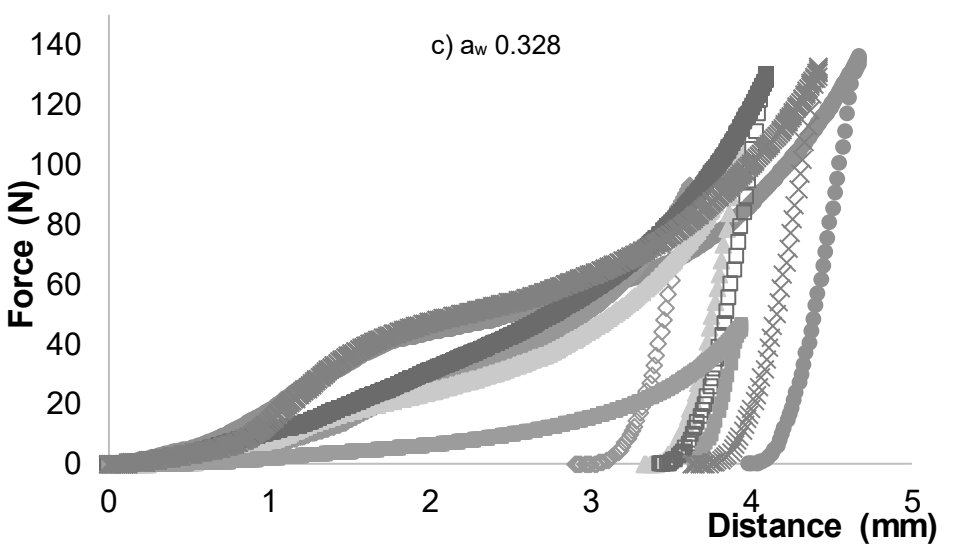
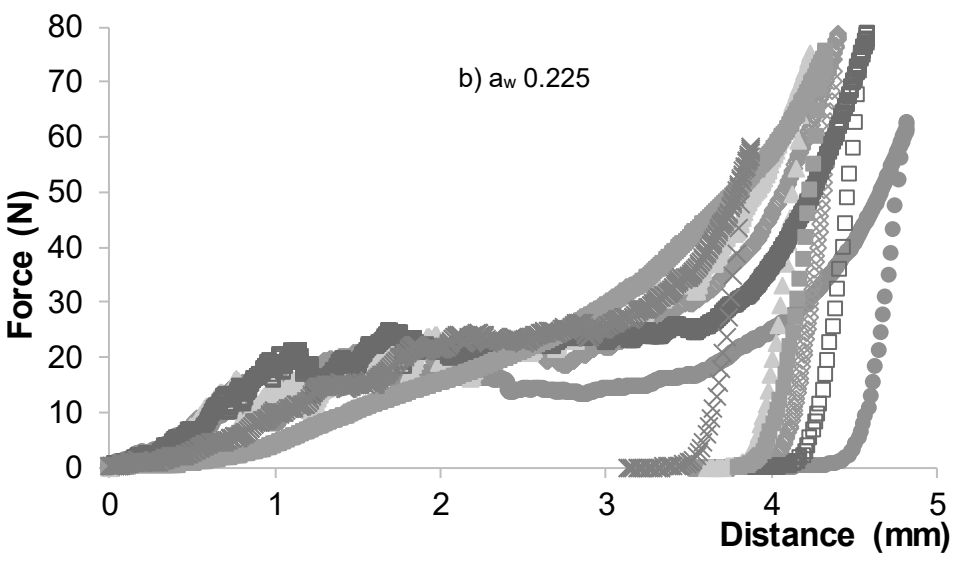
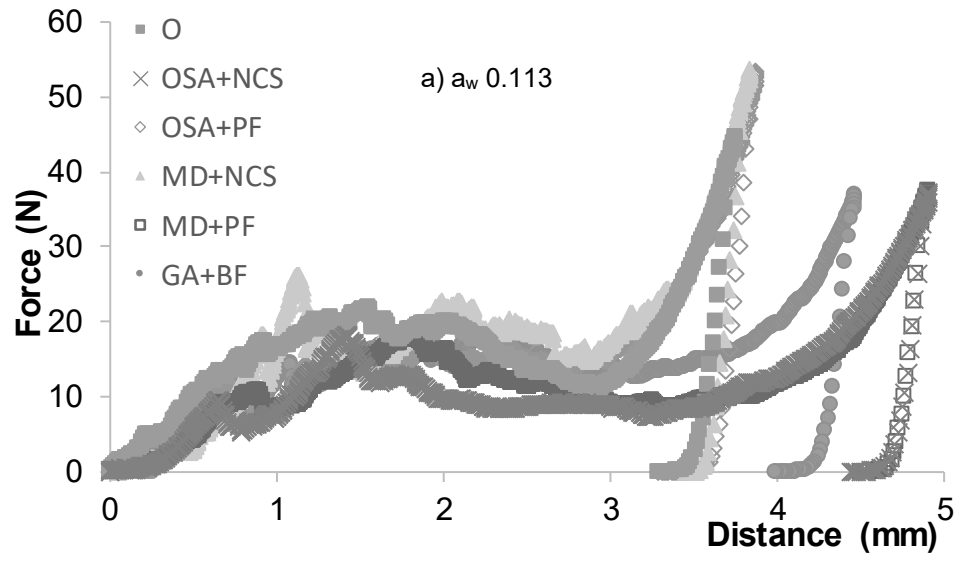


Figure 4

Figure 5

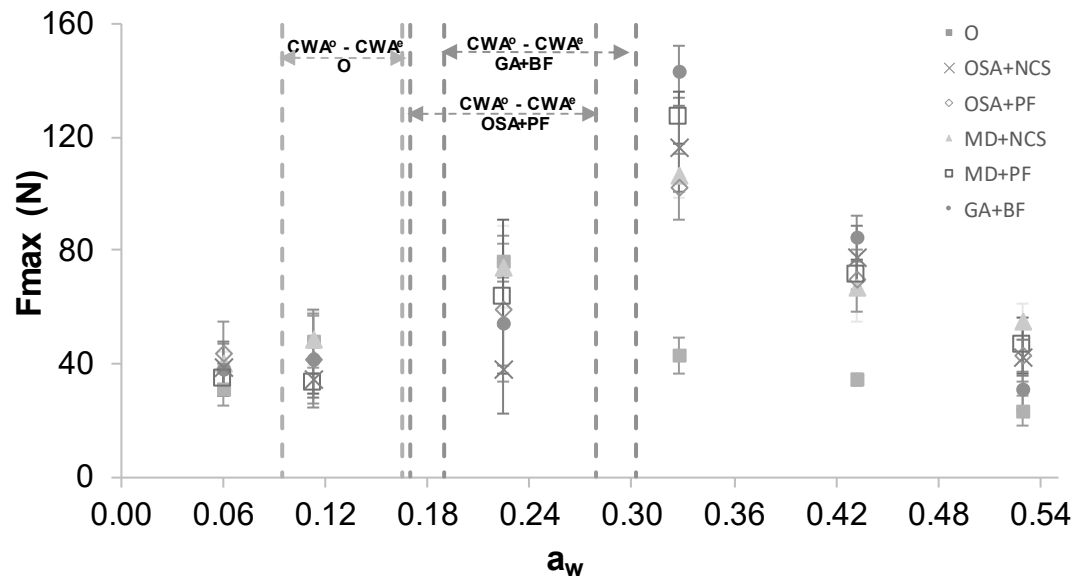


Figure 5

CREDIT AUTHOR STATEMENT

Marilu Andrea Silva-Espinoza: Formal analysis, Funding acquisition, Investigation, Methodology, Writing – original draft, Writing – review & editing.

María del Mar Camacho: Conceptualization, Funding acquisition, Methodology, Project Administration.

Nuria Martínez-Navarrete: Conceptualization, Formal analysis, Funding acquisition, Methodology, Project Administration, Supervision, Writing – original draft, Writing – review & editing.

***Conflict of Interest Form**

The authors have no competing interests to declare